

Reducing inter-pixel crosstalk in HgCdTe detectors

Original

Reducing inter-pixel crosstalk in HgCdTe detectors / Vallone, M.; Goano, M.; Bertazzi, F.; Ghione, G.; Palmieri, A.; Hanna, S.; Eich, D.; Figgemeier, H.. - STAMPA. - 2019-:(2019), pp. 83-84. (Intervento presentato al convegno 19th International Conference on Numerical Simulation of Optoelectronic Devices, NUSOD 2019 tenutosi a Ottawa (Canada) nel 2019) [10.1109/NUSOD.2019.8806849].

Availability:

This version is available at: 11583/2761332 since: 2019-10-18T12:19:40Z

Publisher:

IEEE Computer Society

Published

DOI:10.1109/NUSOD.2019.8806849

Terms of use:

This article is made available under terms and conditions as specified in the corresponding bibliographic description in the repository

Publisher copyright

(Article begins on next page)

Reducing inter-pixel crosstalk in HgCdTe detectors

M. Vallone*, M. Goano*, F. Bertazzi*, G. Ghione*, A. Palmieri*, S. Hanna†, D. Eich†, H. Figgemeier†

* Dipartimento di Elettronica e Telecomunicazioni, Politecnico di Torino, corso Duca degli Abruzzi 24, 10129 Torino, Italy

† AIM Infrarot-Module GmbH, Theresienstraße 2, D-74072 Heilbronn, Germany

E-mail: marco.vallone@polito.it

Abstract—Three-dimensional, realistic full-wave electromagnetic and electrical simulations were done considering a planar HgCdTe 5×5 pixel miniarray with $5 \mu\text{m}$ -wide square pixels, illuminated by narrow Gaussian beams. The results suggest that, by avoiding quasi-neutral regions in the detector's absorber through majority carriers depletion, the inter-pixel crosstalk due to the diffusion of photogenerated carriers is significantly reduced.

I. INTRODUCTION

The II-VI alloy HgCdTe is one of the most versatile materials for the realization of large format infrared (IR) focal plane arrays (FPAs) [1]. Majority carrier depletion of the absorber was indicated as a method to suppress the dark current originating from quasi-neutral regions, reducing the need of expensive cryogenic cooling systems [2], [3]. We show that carrier depletion is also effective to cut down the diffusive inter-pixel crosstalk [4], [5], a deleterious effect due to lateral carrier diffusion in planar FPAs, particularly relevant when the pixel pitch (often $3 - 15 \mu\text{m}$) is much smaller than minority carriers diffusion length (in the orders of tens of micrometers).

II. PHOTODETECTOR STRUCTURE

Fig. 1 shows the photodetector structure: it is a planar 5×5 pixels miniarray with $5 \mu\text{m}$ -wide square pixels with p -on- n doping scheme, consisting in a small modification of a literature example [6], more extensively described in [7]. A narrow-bandgap, low donor-doped and compositionally graded Hg $_{1-x}$ Cd $_x$ Te absorber is connected by two transition layers to two wide-bandgap HgCdTe regions (buffer and cap, Fig. 1(c))

with appropriately chosen doping profile. The absorber's compositional grading makes the detector suitable for both mid wavelength (MWIR, $\lambda \in [3, 5] \mu\text{m}$) and long wavelength (LWIR, $\lambda \in [8, 14] \mu\text{m}$) operation. The HgCdTe properties were described through the models reported in [4], taking into account the composition, doping, and temperature dependence of the HgCdTe alloy. The Shockley-Read-Hall (SRH) recombination processes were modeled as in [8] considering a lifetime around $100 \mu\text{s}$. Fermi-Dirac statistics and incomplete dopant ionization were taken into account.

III. MODELING METHOD

The geometry, doping and composition profiles were defined employing the Sentaurus three-dimensional (3D) numerical simulator by Synopsys [9], also used to perform the electrical simulations in the drift-diffusion approximation. With reference to Fig. 1(a,b), in the present work we defined the inter-pixel crosstalk as the photoresponse of a neighboring pixel (NNs or CNs) to a beam illuminating the central pixel (CP).

In order to obtain the solution of the electromagnetic problem, we sampled the absorber's and the transition regions' composition profiles [7], converting them to staircases of $N = 30$ sublayers, each with uniform value for the complex refractive index $n_r + i\kappa$ according to the sublayer's HgCdTe composition ([4], Table I), as shown in Fig. 1(b,d). With this approach, the EMW commercial simulator [9] was able to solve the electromagnetic problem by a full-wave approach, according to the Finite Differences Time Domain (FDTD) method [10]. The optical generation rate distribution G_{opt} into the pixel due to interband optical absorption was inserted as

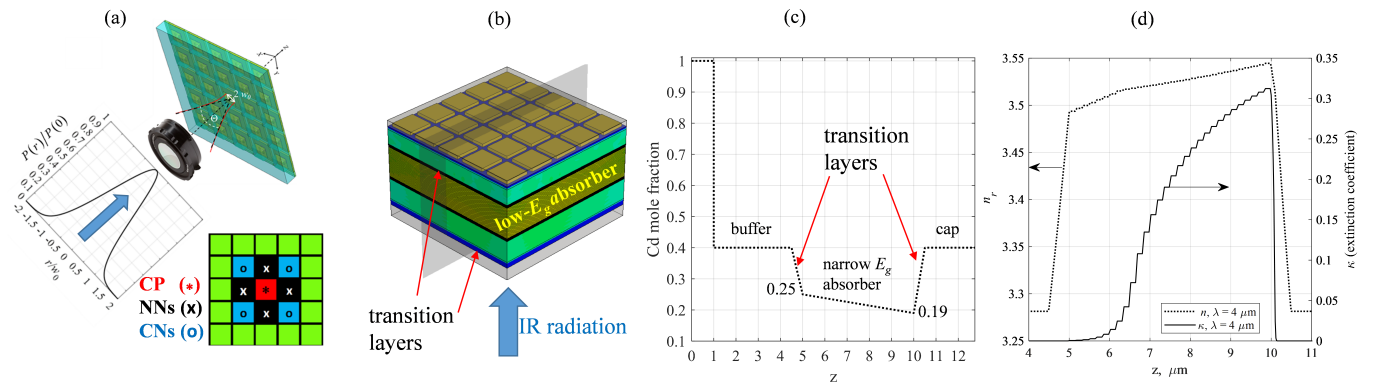


Fig. 1. (a) The 3D miniarray and (b) its Cd mole fraction x of Hg $_{1-x}$ Cd $_x$ Te profile along z (E_g is the bandgap). (c) The discretization of the real n_r and imaginary κ parts of the absorber's refractive index profile along z .

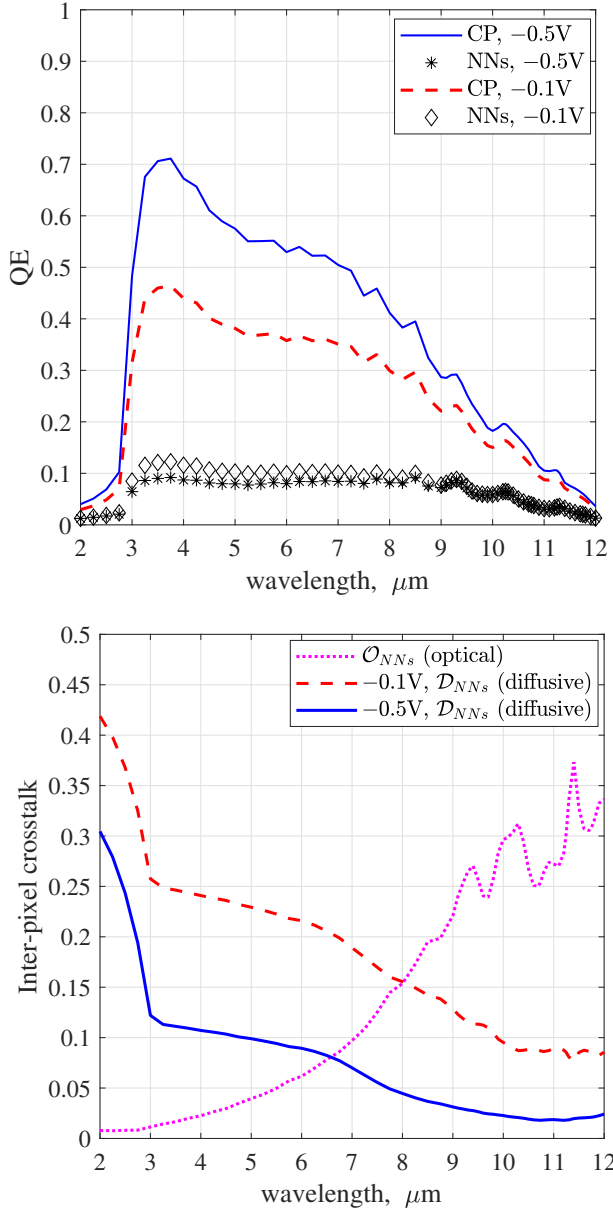


Fig. 2. (a) The CP and NNs spectral QE for the described Gaussian beam illumination centered on the CP, for $T = 140$ K and $V_{\text{bias}} = -0.1$ V and -0.5 V. (b) For the same temperature, the “optical” and “diffusive” inter-pixel crosstalk (adimensional ratios) are shown for $V_{\text{bias}} = -0.1$ V and -0.5 V (the optical crosstalks is bias-independent).

a source term in the drift-diffusion continuity equations after having applied the same reverse bias V_{bias} to all the pixels.

IV. RESULTS, COMMENTS AND CONCLUSIONS

Fig. 2 shows the spectral quantum efficiency QE and the inter-pixel crosstalk at $T = 140$ K for $V_{\text{bias}} = -0.1$ V and -0.5 V for the described illumination, where the definitions for the “optical” \mathcal{O}_{NNs} , “total” \mathcal{C}_{NNs} , and “diffusive” \mathcal{D}_{NNs}

contributions to the crosstalk

$$\mathcal{O}_{NNs} = \frac{\int_{V_{NNs}} G_{\text{opt}}(x, y, z) dx dy dz}{\int_{V_{CP}} G_{\text{opt}}(x, y, z) dx dy dz} \quad (1)$$

$$\mathcal{C}_{NNs} = \frac{I_{ph, NNs}}{I_{ph, CP}}, \quad \mathcal{D}_{NNs} \approx \mathcal{C}_{NNs} - \mathcal{O}_{NNs} \quad (2)$$

have been introduced (I_{ph} is the photocurrent, V_{CP} and V_{NNs} are the CP and NNs pixel volumes). By increasing the reverse bias from -0.1 V to -0.5 V, the carrier depletion in the absorber increases significantly, allowing a larger fraction of photogenerated carriers to drift towards the CP contact, before they diffuse laterally: this is pretty apparent comparing the dashed and solid lines in Fig. 2(a,b), referred to -0.1 V and -0.5 V respectively. The moderate electrical field in the absorber that originates from the depletion of the majority carriers is enough to curtail the inter-pixel “diffusive” crosstalk even at moderate reverse bias. Beside the ensuing Auger suppression [3], this is an additional advantage of carrier-depleted detectors. Further investigations will cover the response to non-monochromatic illumination [11], [12], considering different and higher values of temperature, and characterizing the effect of the absorber’s background doping.

REFERENCES

- [1] M. A. Kinch, “The future of infrared; III-Vs or HgCdTe?” *J. Electron. Mater.*, vol. 44, no. 9, pp. 2969–2976, 2015.
- [2] —, “Fundamental physics of infrared detector materials,” *J. Electron. Mater.*, vol. 29, no. 6, pp. 809–817, 2000.
- [3] J. Schuster, R. DeWames, and P. S. Wijewarnasuraya, “Dark currents in a fully-depleted LWIR HgCdTe *P-on-n* heterojunction: analytical and numerical simulations,” *J. Electron. Mater.*, vol. 46, no. 11, pp. 6295–6305, 2017.
- [4] M. Vallone, M. Goano, F. Bertazzi, G. Ghione, W. Schirmacher, S. Hanna, and H. Figgemeier, “Simulation of small-pitch HgCdTe photodetectors,” *J. Electron. Mater.*, vol. 46, no. 9, pp. 5458–5470, 2017.
- [5] M. Vallone, M. Goano, F. Bertazzi, G. Ghione, S. Hanna, D. Eich, and H. Figgemeier, “Diffusive-probabilistic model for inter-pixel crosstalk in HgCdTe focal plane arrays,” *IEEE J. Electron Devices Soc.*, vol. 6, no. 1, pp. 664–673, 2018.
- [6] A. Rogalski, M. Kopytko, and P. Martyniuk, “Performance prediction of p-i-n HgCdTe long-wavelength infrared HOT photodiodes,” *Appl. Opt.*, vol. 57, no. 18, pp. D11–D18, 2018.
- [7] M. Vallone, M. Goano, F. Bertazzi, G. Ghione, S. Hanna, D. Eich, and H. Figgemeier, “FDTD simulation of compositionally graded HgCdTe photodetectors,” *Infrared Phys. Tech.*, vol. 97, pp. 203–209, 2019.
- [8] M. Vallone, M. Mandurrino, M. Goano, F. Bertazzi, G. Ghione, W. Schirmacher, S. Hanna, and H. Figgemeier, “Numerical modeling of SRH and tunneling mechanisms in high-operating-temperature MWIR HgCdTe photodetectors,” *J. Electron. Mater.*, vol. 44, no. 9, pp. 3056–3063, 2015.
- [9] *Sentaurus Device User Guide. Version M-2017.09*, Synopsys, Inc., Mountain View, CA, Sept. 2017.
- [10] J.-P. Berenger, “A perfectly matched layer for the absorption of electromagnetic waves,” *J. Comp. Phys.*, vol. 114, no. 2, pp. 185–200, 1994.
- [11] M. Vallone, A. Palmieri, M. Calciati, F. Bertazzi, F. Cappelluti, G. Ghione, M. Goano, S. Hanna, H. Figgemeier, R. Scarmozzino, E. Heller, and M. Bahl, “Broadband 3D optical modeling of HgCdTe infrared focal plane arrays,” in *17th International Conference on Numerical Simulation of Optoelectronic Devices (NUSOD 2017)*, Copenhagen, Denmark, July 2017, pp. 205–206.
- [12] M. Vallone, A. Palmieri, M. Calciati, F. Bertazzi, F. Cappelluti, G. Ghione, M. Goano, M. Bahl, E. Heller, R. Scarmozzino, S. Hanna, D. Eich, and H. Figgemeier, “Non-monochromatic 3D optical simulation of HgCdTe focal plane arrays,” *J. Electron. Mater.*, vol. 47, no. 10, pp. 5742–5751, 2018.